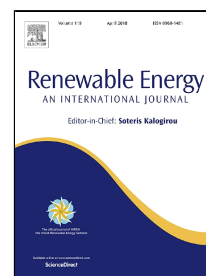


Accepted Manuscript

Performance of an unglazed transpire collector in the facade of a building for heating and cooling in combination with a desiccant evaporative cooler

F. Peci, F. Comino, M. Ruiz de Adana



PII: S0960-1481(18)30029-6
DOI: 10.1016/j.renene.2018.01.029
Reference: RENE 9634
To appear in: *Renewable Energy*
Received Date: 07 August 2017
Revised Date: 08 January 2018
Accepted Date: 11 January 2018

Please cite this article as: F. Peci, F. Comino, M. Ruiz de Adana, Performance of an unglazed transpire collector in the facade of a building for heating and cooling in combination with a desiccant evaporative cooler, *Renewable Energy* (2018), doi: 10.1016/j.renene.2018.01.029

This is a PDF file of an unedited manuscript that has been accepted for publication. As a service to our customers we are providing this early version of the manuscript. The manuscript will undergo copyediting, typesetting, and review of the resulting proof before it is published in its final form. Please note that during the production process errors may be discovered which could affect the content, and all legal disclaimers that apply to the journal pertain.

Performance of an unglazed transpire collector in the facade of a building for heating and cooling in combination with a desiccant evaporative cooler

F. Peci*, F. Comino, M. Ruiz de Adana

fernando.peci@uco.es, francisco.comino@uco.es, manuel.ruiz@uco.es

Departamento de Química-Física y Termodinámica Aplicada, Escuela Politécnica Superior, Universidad de Córdoba, Campus de Rabanales, Antigua Carretera Nacional IV, km 396, 14072 Córdoba, Spain

Abstract

Refurbishment of energy inefficient buildings is an effective way of reducing energy consumption in urban areas. This can be done by taking advantage of the renewable energy sources available, mainly, solar energy. Desiccant evaporative cooling combined with unglazed transpired collectors, UTC's, allows covering the heating demand in the cold season and cooling demand in the hot season. UTC's can be installed on the facades of buildings, meeting a double goal: refurbishing the building exterior and providing heating and cooling to indoor spaces. In this paper, a model of this system was implemented using TRNSYS and the energy savings obtained were evaluated in different climatic conditions, different façade orientations and different building shapes. The objective was to find the best conditions to install this system and estimating the energy savings that can be reached, and its costs. The results showed that the reduction of heating demand was possible in all climatic conditions, weakly depending on the shape and orientation of the UTC façade installed. Cooling was also possible, but it depended more on the shape of the building. The higher energy savings were found for the linear shape buildings. Therefore, refurbishment using a UTC façade could be an interesting alternative for energy saving throughout the year in these cases.

Keywords: Desiccant evaporative cooling, unglazed solar collector, ventilated façade, building energy saving, solar façade.

Nomenclature

A_c collector area (m^2)

C_A cost of the UTC façade per unit area ($€ m^{-2}$)

C_E initial cost of the UTC installation apart from cost per unit area ($€$)

C_F fuel cost ($€ kWh^{-1}$)

c_p specific heat ($J kg^{-1} K^{-1}$)

E_{del} heating or cooling energy delivered (kWh)

E_{elec} electrical energy used (kWh)

F fraction of heating or cooling load covered by solar energy

F_{cg} collector to ground view factor

- 39 F_{cs} collector to sky view factor
- 40 I_c total solar insolation incident on the collector ($W m^{-2}$)
- 41 L heating of cooling load in a year (kWh)
- 42 LCS Life Cycle Savings (€)
- 43 P_1 ratio of life cycle fuel savings to first-year fuel savings
- 44 P_2 ratio of life cycle capital expenditures to initial investment
- 45 Q_{conv} collector convective heat loss (W)
- 46 Q_{rad} collector radiant heat loss (W)
- 47 T_{amb} ambient temperature ($^{\circ}C$)
- 48 T_{coll} collector temperature (K)
- 49 T_{gnd} ground temperature (K)
- 50 T_{out} collector output temperature ($^{\circ}C$)
- 51 T_{pi} process inlet temperature ($^{\circ}C$)
- 52 T_{po} process output temperature ($^{\circ}C$)
- 53 T_{ri} regeneration inlet temperature ($^{\circ}C$)
- 54 T_{sky} sky temperature (K)
- 55 U_{∞} free stream velocity ($m s^{-1}$)
- 56 W Collector width (m)
- 57 α_c collector absorptance
- 58 ϵ_c absorber surface emissivity
- 59 v_0 suction velocity ($m s^{-1}$)
- 60 v velocity normal to the wall ($m s^{-1}$)
- 61 ρ density ($kg m^{-3}$)
- 62 σ Stefan-Boltzmann constant ($W m^{-2} K^{-4}$)
- 63 ω_{pi} process inlet humidity ratio ($g kg^{-1}$)
- 64 ω_{po} process output humidity ratio ($g kg^{-1}$)
- 65 ω_{ri} regeneration inlet humidity ratio ($g kg^{-1}$)
- 66 Ω flow rate ($m^3 h^{-1}$)

67

68

69

1. Introduction

Building energy consumption reaches approximately 40 % of the total energy used in a country [1]. Air conditioning and heating systems account for most of this energy. Many old buildings have a poor thermal performance, either in the cold and the hot season. There exist entire neighbourhoods with this thermal inefficient buildings and bad conditioned spaces in most big towns and cities. Therefore, decreasing energy inefficiency and increasing the quality of life in these neighbourhoods not only reduces the energy consumption but benefits communities.

Trying to improve conditioned spaces without increasing the energy demand could require the use of all the renewable energy sources available. In the case of buildings, the major renewable energy source is solar energy, as they have large surface areas exposed to solar radiation. Solar collectors can take advantage of this in many ways: photovoltaic panels, thermal glazed collectors and special types of facades [2,3]. Refurbishment of deteriorated buildings with facades that could improve its energy performance could be a possible solution to the building energy inefficiency problem.

There are many types of collectors that absorb solar radiation to be used in heating or cooling systems [4]. Thermal solar collectors are usually installed to get domestic hot water, although there are also absorption cycle systems that use solar energy totally or partially for cooling [5]. The most efficient collectors are glazed solar collectors [6], and they are usually installed on the roof of buildings [7]. A typical arrangement for a glazed solar collector can be seen in figure 1. However, installing this kind of collectors on facades presents some problems as its weight, maintenance and space occupied. Another cooling system that uses heating as primary energy source is desiccant evaporative cooling (DEC). The conventional cycle of this system can be seen in figure 2. This system can use the heat absorbed, for instance by thermal solar collectors, to regenerate a desiccant device, usually a desiccant wheel, although a liquid desiccant can also be used [8].

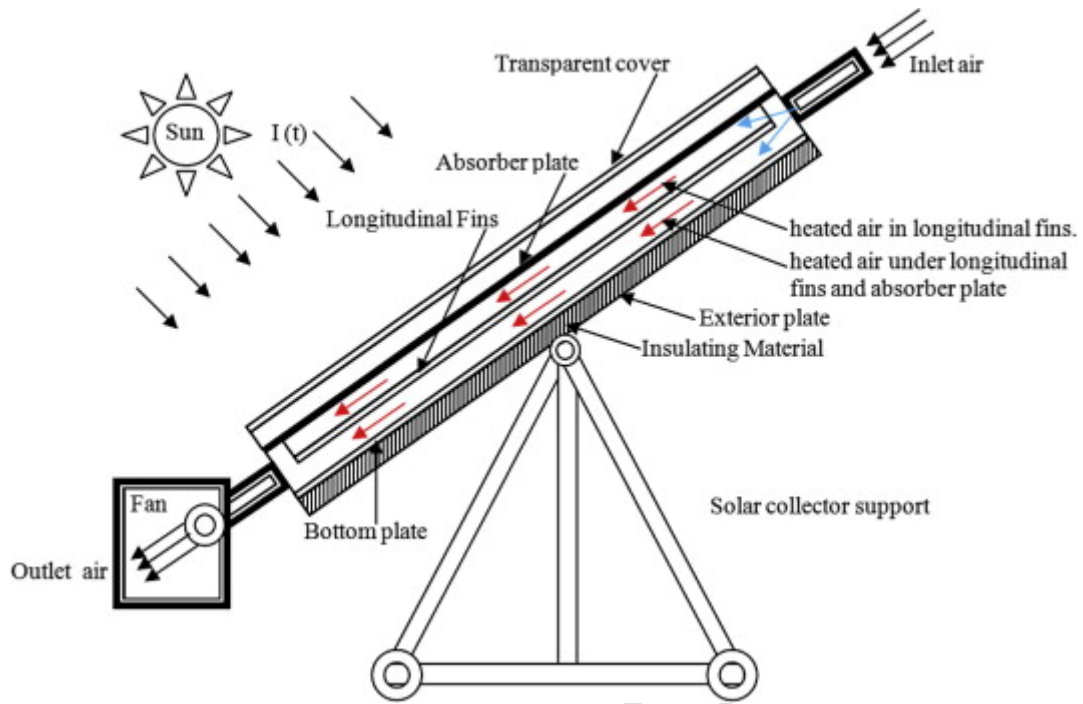


Figure 1. Typical glazed solar air heater [9].

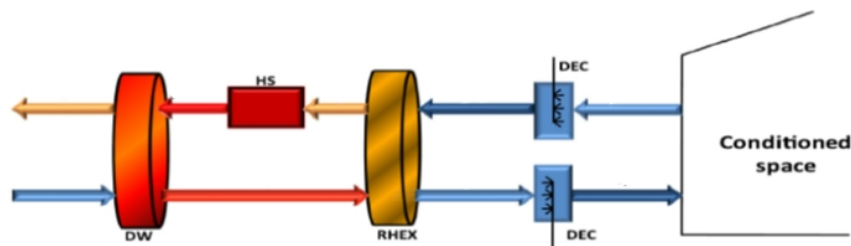


Figure 2. Schematic of a conventional desiccant cooling system [10], where HS is a heater system, DEC's are direct evaporative coolers, DW is a desiccant wheel and RHEX is a rotary heat exchanger.

Ventilated facades have been studied in the last few years as an alternative for installing solar collectors on building facades [11]. Ventilated facades take ambient air from the outside and heat it before introducing it into the building. Ventilated facades are divided into two categories: glazed and opaque. Double glazed facades absorb solar radiation with a shading layer which is situated between two glazed layers, see figure 3, whereas opaque facades absorb energy through its outer layer, which is opaque, and transfer it to the air circulating through the adjacent air gap, as it can be seen in figure 4. The hot air is then introduced into the space to be conditioned in the cold season or exhausted to the outside to prevent overheating in the hot season. The most efficient opaque solar collectors are the unglazed transpire collectors, UTC [12]. UTC's can be easily installed on façade and are inexpensive, making it a good alternative as a solar façade [13, 14, 15]. In figure 5 an example of refurbishment with UTC is shown. There are also many examples of UTC façade buildings in the industry [16].

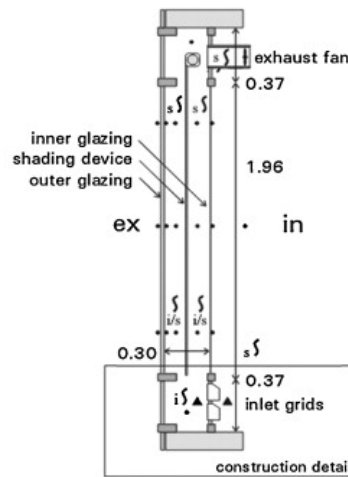


Figure 3. Schematic of a typical double glazed façade [17].

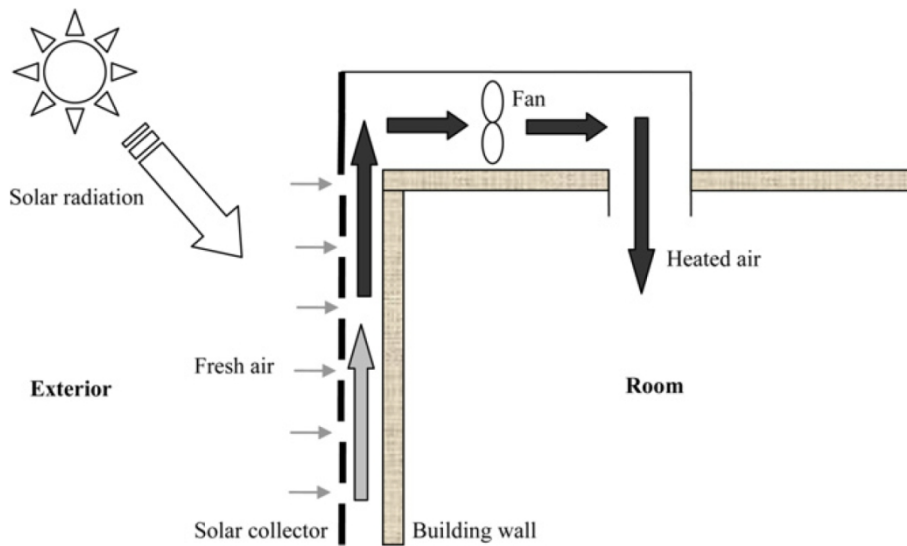


Figure 4. Schematic of a typical opaque ventilated façade [18].

Solar collectors can be used to regenerate a desiccant wheel [19]. The hot air from an UTC can be also used in the hot season combined with a DEC system, figure 6. Other authors have studied the potential of using an UTC as a heat source for DEC. In [6], the thermal performance of this combination was studied. It was concluded that using a UTC regeneration for a DEC system is an attractive alternative to glazed collectors, mainly due to its lower cost. However, it also reached the conclusions that, firstly, the effectiveness obtained is lower than that of a glazed collector, as the inlet air cannot be preheated in a UTC, and secondly, the area needed for the same performance is greater for an unglazed collector. However, the cooling demand coverage of a building was not studied in this piece of work, and there is no information about the climates in which UTC's have a better performance. In another study, [20] showed that desiccant wheel can work satisfactorily with low regeneration air temperature. Regarding heating with

UTC's, many authors have studied its potential for building heating and industry drying processes [21].



Figure 5. Building facade renovated with UTC panels [14].

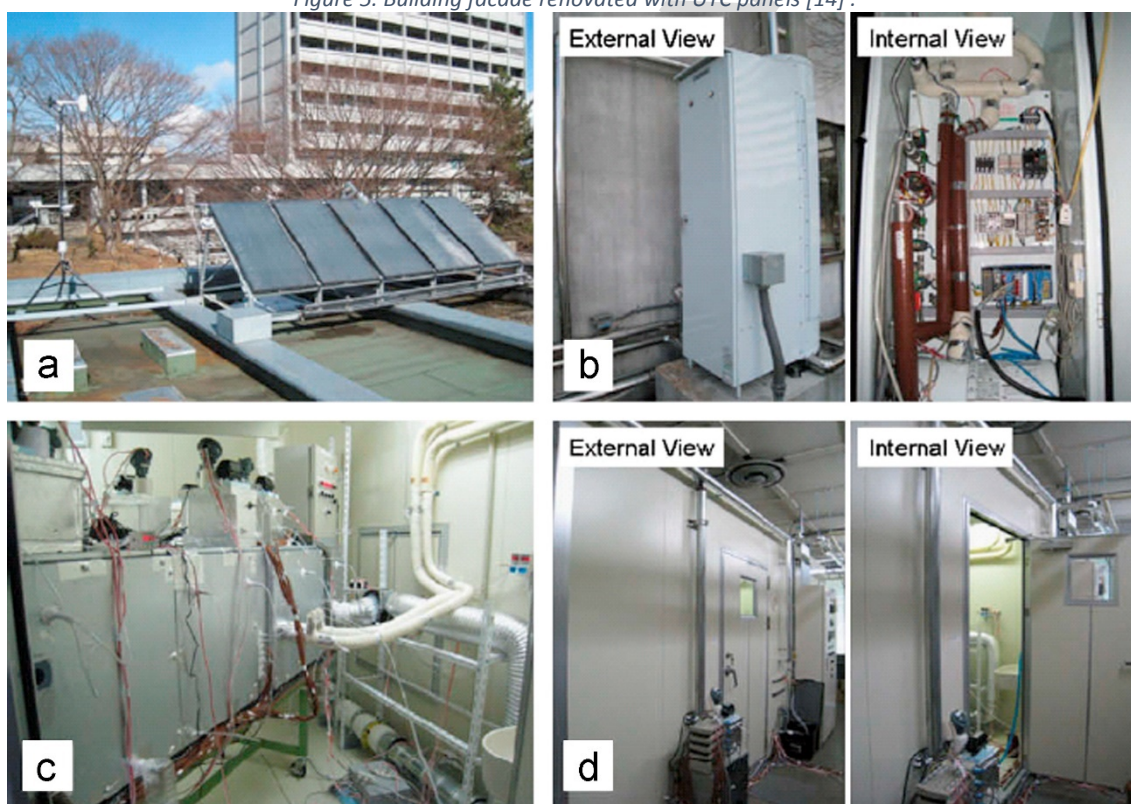


Figure 6. Example of a real desiccant evaporative cooling system [22]: (a) solar collector; (b) thermal storage and auxiliary heater; (c) desiccant cooling; (d) controlled chambers.

The objective of this piece of work was to show that heating and cooling can be achieved by building refurbishment installing UTC based facades, and to estimate the percentage of heating and cooling demand coverage that can be obtained with this system. In this paper a DEC system with desiccant wheel and UTC modules installed on the façade of a

building was studied through numerical simulations for the cooling and the heating season. In the hot season, cooling was achieved with the DEC system, whereas hot air was supplied directly from the UTC's outlet air in the cold season. The advantages and disadvantages in both seasons were studied in four locations around a typical meteorological year from the economic and energetic points of view. This system was proposed as a refurbishment measure to renew degraded buildings.

2. Methodology

In this section the numerical models for the different components of the desiccant evaporative cooling system are presented. These models were implemented in the transient building simulation software TRNSYS, and a series of simulations was run to evaluate the energy savings in different building shapes under several climatic conditions. The cost analysis methodology is also explained.

2.1 The evaporative desiccant system

The arrangement showed in figure 7 was used for this study. It was based on the Pennington Cycle [23]. This configuration has also been used with other heat sources [24]. In this case, it consisted of a UTC façade as regeneration air heat source, a desiccant wheel (DW), a rotary heat exchanger (RHE), and two direct evaporative coolers (EC). The process air, state 1, is firstly introduced in the desiccant wheel to remove most of its moisture content, state 2. Then, the adsorption heat generated in this process is partly transferred to the exhaust air in an rotary heat exchanger, state 3. Finally, the air is cooled and humidified in the EC before entering the room, state 4. The building exhaust air, state 5, is cooled with another EC and then, state 6, introduced in the RHE to remove cool from the process air, state 7. The ambient air, state 1, passed through the holes of the UTC where it is heated, state 8, and then is introduced in the DW regeneration section, and, after this, is exhausted. In figure 8, the air states of the process and regeneration air streams are shown in a psychrometric chart. It can be seen that the dehumidification process carried out by the DW, process 1-2, allows the process air to be cooled by the EC below the incoming air dew temperature. The advantage of this system is that the evaporative cooling process is enhanced, since the incoming air is drier. The psychrometric chart also shows that the heating due to the adsorption process is almost as much as the cooling in the evaporative coolers, see process 3-4.

The set temperatures for the indoor spaces were 21 °C in the heating season and 25 °C in the cooling season. Relative humidity was set to 50% in both seasons.

188

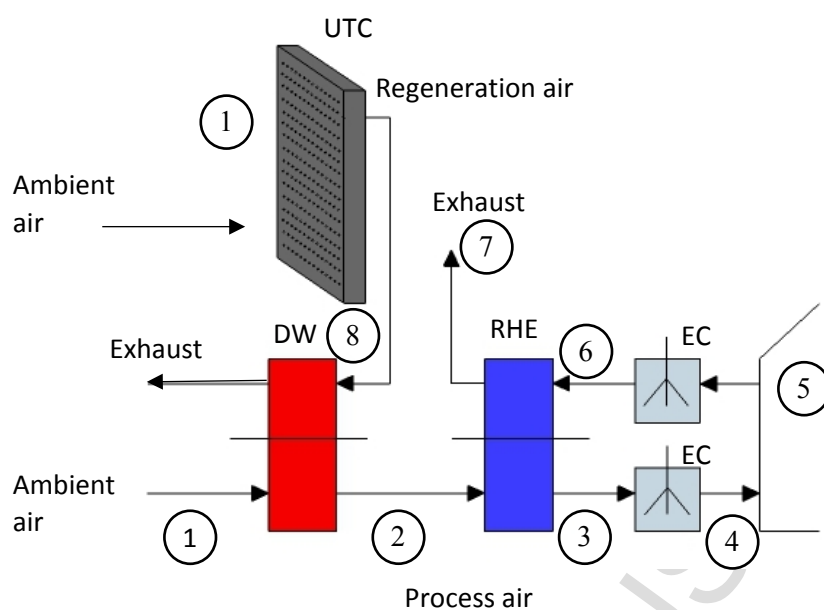
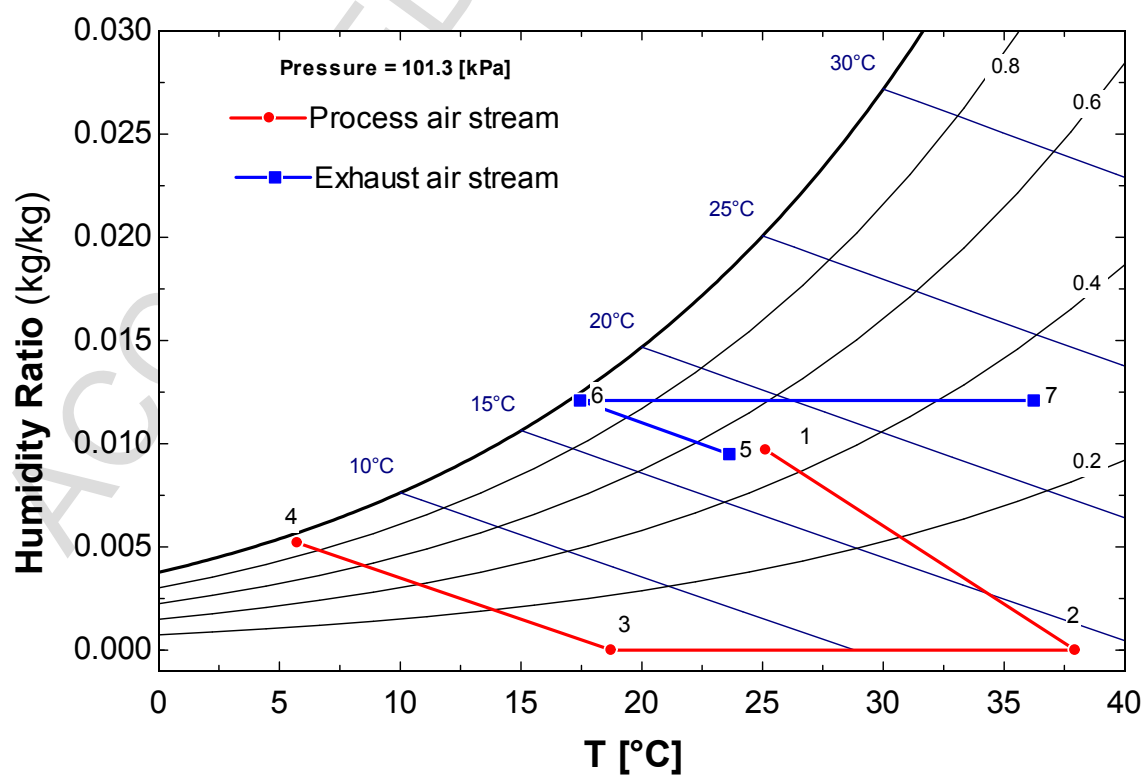


Figure 7. DEC-UTC System layout.



196

Figure 8. Process and regeneration air states in the DEC system for a typical summer day in Vienna. States 1 – 7 are the states corresponding to process air flow and regeneration air flow in figure 7.

2.2 The UTC facade

The UTC was made up of a perforated metal absorption layer, a plenum, an insulation layer and a set of ducts to distribute the heated air directly to the building or to the DEC. The UTC's absorber layer consists of a 1 mm thick galvanized steel layer highly perforated, so it can be assimilated to a porous layer. A schematic of the basic UTC module can be seen in figure 9. Equations 1 to 3 were used to model the UTC, they were extracted from [12].

$$\rho c_p v_0 A_c (T_{out} - T_{amb}) = I_c A_c \alpha_c - Q_{rad} - Q_{conv} \quad (1)$$

$$Q_{rad} = \epsilon_c \sigma A_c (T_{coll}^4 - F_{cs} T_{sky}^4 - F_{cg} T_{gnd}^4) \quad (2)$$

$$Q_{conv} = 0.82 \left(\frac{U_{\infty} v}{v_0^2} \right) W [\rho c_p v_0 (T_{coll} - T_{amb})] \quad (3)$$

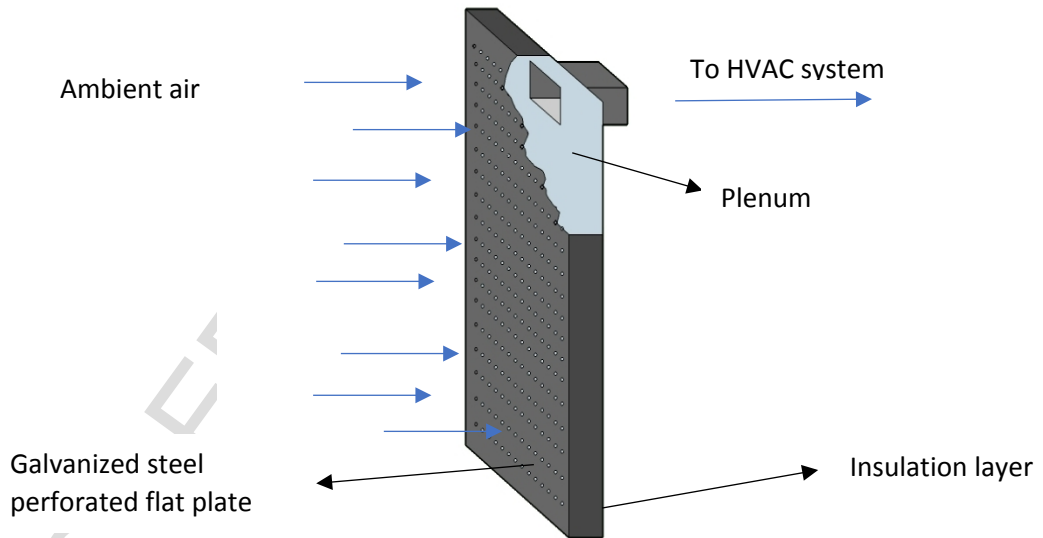


Figure 9. Schematic of a UTC module

The advantage of the porous system is its ability to absorb the thermal boundary layer so the convection losses are minimized provided that the approaching velocity is adequate. In this study the air flow rate through the UTC modules was considered constant during the working

time, with a value of 2300 m³/h, according to regulations [25]. The façade was partitioned according to storeys, each of which had its own set of fans. The efficiency of the UTC façade can be evaluated using equation (4) [12]:

$$\eta = \frac{\rho C_p v_0 (T_{coll} - T_{amb})}{I_c} \quad (4)$$

2.3 Desiccant Wheel

The empirical model of a desiccant wheel that was developed and validated in [26] was used in this study. This model was based on the design of experiment methodology and it was focused in the performance of a silica gel DW activated using low temperature regeneration air. The authors adjusted a set of polynomials of the form shown in equation 5 to the empirical results of a series of experimental tests carried out in a set of process air and regeneration air conditions. The list of parameters obtained empirically from these experiments can be seen in table 1. These parameter allow to evaluate the process air output temperature and humidity using the process and regeneration temperature and humidity input values.

$$\hat{Y} = b_0 + \sum_{i=1}^k b_i X_i + \sum_{i=1}^k b_{ii} X_i^2 + \sum_{i=1}^{k-1} \sum_{j=i+1}^k b_{ij} X_i X_j \quad (5)$$

Table 1. Estimated parameters for equation 5, obtained from experimental results in [26] using the design of experiment methodology.

Estimated parameters	X_i	$T'_{po} \times 10^3$ [°C]	$\omega'_{po} \times 10^3$ [g kg ⁻¹]	Estimated parameters	X_i	$T'_{po} \times 10^3$ [°C]	$\omega'_{po} \times 10^3$ [g kg ⁻¹]
b_0	-	-6736.67	-15366.80	b_{11}	ω_{pi}^2	-17.23	16.76
b_1	T_{pi}	72.10	1277.57	b_{12}	$\omega_{pi} \cdot T_{ri}$	-1.49	-2.23
b_2	ω_{pi}	772.28	-785.18	b_{13}	$\omega_{pi} \cdot \omega_{ri}$	5.65	16.84
b_3	T_{ri}	410.38	1310.33	b_{14}	$\omega_{pi} \cdot \Omega_{pi}$	20.50	-6.79
b_4	ω_{ri}	224.17	-916.88	b_{15}	T_{ri}^2	-5.09	-11.90
b_5	Ω_{pi}	357.36	-94.71	b_{16}	$T_{ri} \cdot \omega_{ri}$	7.31	-10.40
b_6	T_{pi}^2	16.58	-28.38	b_{17}	$T_{ri} \cdot \Omega_{pi}$	6.71	-3.50
b_7	$T_{pi} \cdot \omega_{pi}$	-14.35	29.84	b_{18}	ω_{ri}^2	-9.72	24.41
b_8	$T_{pi} \cdot T_{ri}$	7.35	-10.61	b_{19}	$\omega_{ri} \cdot \Omega_{pi}$	-5.49	11.88
b_9	$T_{pi} \cdot \omega_{ri}$	-12.93	6.35	b_{20}	Ω_{pi}^2	-12.17	-9.44
b_{10}	$T_{pi} \cdot \Omega_{pi}$	-8.71	5.89	-	-	-	-

2.4 Evaporative coolers and rotary heat exchanger

The RHE and the EC's were modeled using the standard TRNSYS types 760 and 506 [27]. The RHE was set with a sensible effectiveness of 0.93 [28], and the evaporative coolers with a saturation efficiency of 0.95 [29].

2.5 Building model

A set of building models were created using TRNBUILD to simulate the performance of the UTC façade system as heating system in the winter [30] and together with the DEC in the summer. The set of simulations was created with a unique indoor thermal node [31], considering the

influence of the volume to surface ratio by studying different building shapes. Three shapes were selected: compact, linear and tower. The volume was 1300 m³ for all cases. These shapes and their dimensions can be seen in figure 10. The area of the façade surfaces and the percentage covered with UTC are shown in table 2.

The original façade layers were those of a traditional façade. The materials and geometry can be seen in table 3. The four building facades had a 25% of window surface [32]. The window's panel had an U-value of 3.21 W/m²K and a g-value of 0.772 [27]. Although in this model a unique thermal zone was considered, a number of inner walls were modeled to account for their thermal capacity. Two models were tested for comparison: the original building, and a refurbished building covering a 75% of the façade with UTC's. North, south, east and west UTC façade orientations were tested in order to evaluate the accommodation of solar energy availability to occupation schedule.

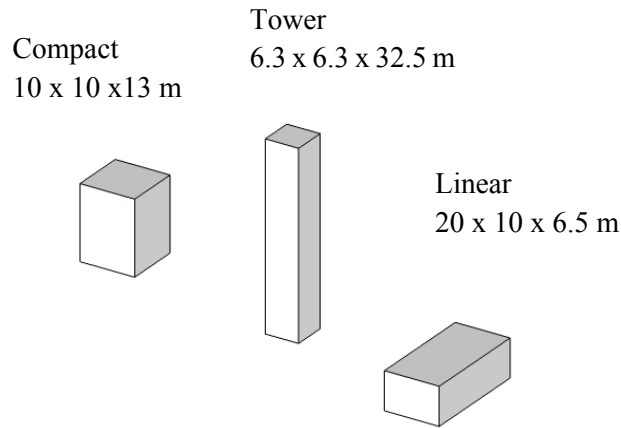


Figure 10. Building shapes.

Table 2. Surface areas of the buildings.

Shape	Façade area (m ²)	Area covered with UTC (m ²)	Window area (m ²)
Linear	130	97.5	32.5
Compact	130	97.5	32.5
Tower	204.8	153.6	51.2

Table 3. Layers and properties of the previous façade.

Layer	Material	Thickness (m)	Conductivity (W/m K)	Heat capacity (kJ/kg K)	Density (kg/m ³)
1 (inside)	Plaster	0.01	0.300	1.00	900
2	Brick	0.14	0.760	1.00	1600
3	Insulation	0.05	0.034	1.45	25
4	Air gap	0.18	0.090(resistance m ² K/W)	-	-
5(outside)	Hollow brick	0.05	0.810	0.92	1700

An office schedule was selected, from 9:00 a.m. to 6:00 p.m. with an occupation of 44 people, seated and writing according to ISO 7730. Lights were on at working time with a total heat gain of 10 W/m² and also 30 computers with a power of 230 W each. The building was not occupied on weekends.

2.6 Climates

The simulations were carried out under four different climates according to [33], that correspond to dry and mild, wet and hot, dry and hot, and wet and mild summer climate conditions. The locations selected were Vienna, Cairo, Athens and Honolulu, see table 4. Typical meteorological data from Meteonorm [34] database were used.

Table 4. Locations selected and their climatic conditions.

Location	Climate	Summer Temperatures	Summer Humidity
Vienna	Moderate	Mild	Dry
Cairo	Hot continental	Hot	Dry
Athens	Mediterranean	Hot	Wet
Honolulu	Subtropical	Mild	Wet

2.7 Simulation case studies

The transient building simulation software TRNSYS [27] was used for the simulations. A timestep of 1 hour was set, and simulations were run for a typical meteorological year in each climate. A total of 48 simulations were carried out, combining the building shape, the location and the orientation of the UTC façade. Table 5 shows the list of cases simulated.

Table 5. Simulation cases depending on city, shape of the building and orientation of the UTC façade.

Num.	Location	Shape	Or.	Num.	Location	Shape	Or.	Num.	Location	Shape	Or.	Num.	Location	Shape	Or.
1	Vienna	Linear	N	13	Cairo	Linear	N	25	Athens	Linear	N	37	Honolulu	Linear	N
2	Vienna	Linear	S	14	Cairo	Linear	S	26	Athens	Linear	S	38	Honolulu	Linear	S
3	Vienna	Linear	E	15	Cairo	Linear	E	27	Athens	Linear	E	39	Honolulu	Linear	E
4	Vienna	Linear	W	16	Cairo	Linear	W	28	Athens	Linear	W	40	Honolulu	Linear	W
5	Vienna	Compact	N	17	Cairo	Compact	N	29	Athens	Compact	N	41	Honolulu	Compact	N
6	Vienna	Compact	S	18	Cairo	Compact	S	30	Athens	Compact	S	42	Honolulu	Compact	S
7	Vienna	Compact	E	19	Cairo	Compact	E	31	Athens	Compact	E	43	Honolulu	Compact	E
8	Vienna	Compact	W	20	Cairo	Compact	W	32	Athens	Compact	W	44	Honolulu	Compact	W
9	Vienna	Tower	N	21	Cairo	Tower	N	33	Athens	Tower	N	45	Honolulu	Tower	N
10	Vienna	Tower	S	22	Cairo	Tower	S	34	Athens	Tower	S	46	Honolulu	Tower	S
11	Vienna	Tower	E	23	Cairo	Tower	E	35	Athens	Tower	E	47	Honolulu	Tower	E

12	Vienna	Tower	W	24	Cairo	Tower	W	36	Athens	Tower	W	48	Honolulu	Tower	W
----	--------	-------	---	----	-------	-------	---	----	--------	-------	---	----	----------	-------	---

The seasonal performance factor, SPF , was evaluated for the heating and cooling season in order to compare the performance in the different cases. Its expression is shown in equation 6.

$$SPF = \frac{E_{del}}{E_{elec}} \quad (6)$$

Where E_{del} is the heating or cooling energy delivered and E_{elec} is the electrical energy used.

2.8 Cost analysis

The life cycle savings will be evaluated for all cases in order to obtain the most adequate combination of location, building shape and UTC façade orientation, to minimize the payback period. The life cycle saving is evaluated using equation 7.

$$LCS = P_1 C_F L F - P_2 (C_A A + C_E) \quad (7)$$

Where LCS is the life cycle savings, C_F is the unit cost of delivered conventional energy for the first year of analysis, L is the averaged cooling or heating load, F is the fraction of thermal load covered through solar energy, C_A is the cost of UTC façade per unit area, A is the area of the UTC façade, C_E is the fixed cost of the rest of the UTC installation, and P_1 and P_2 are factors that represent the actualization of the cost of energy and the investment to the present time.

If the LCS value is positive, then the investment is recovered, being the payback period in years equal to the P_1/P_2 ratio, see equation 8 [37]. The greater the P_1/P_2 ratio, the worse the investment in an UTC solar façade.

$$P_1/P_2 = (C_A A + C_E) / C_F L F \quad (8)$$

The price of primary energy was estimated 0.10 €/kWh and a natural gas furnace efficiency of 90 % was selected for the study [37].

3 Results

3.1 UTC Efficiency

The annual average efficiency of the UTC façade is shown in figure 11 for all 48 cases. The highest values were found in cases 27 and 32, corresponding to Athens, in linear west orientation and compact east orientation, respectively. On the other hand, the lowest values were found in cases 9, 21 and 33, corresponding to Vienna, Cairo and Athens north orientation.

North orientation presented the lower values for all the locations; for this orientation the lowest values were found for the tower case in every location. South orientation showed similar values, around 45%, for linear and compact shapes in all locations, whereas in tower shape the efficiency was around 29% for all locations. The value for east orientation was the highest for Vienna, Athens and Honolulu, linear shape. For west orientation the highest efficiency values were found in Cairo, linear shape, Athens and Honolulu, compact shape.

Similar values were found in [6], where a single unglazed solar collector was studied. Although these values were lower than that for glazed collector, the advantages aforementioned and the possibility of installing them as part of the façade of a building make UTC façade a viable method of solar radiation absorption for its use in thermal systems.

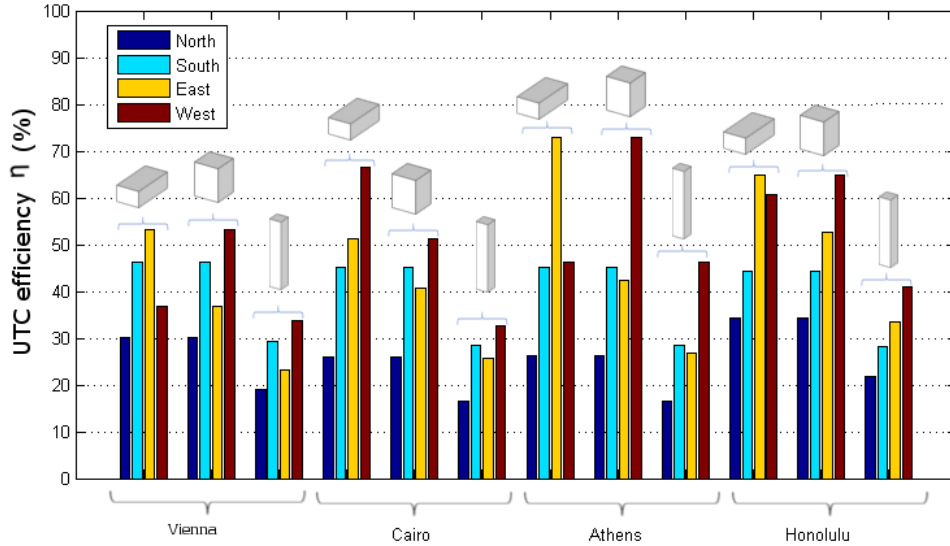


Figure 11. UTC efficiency mean values in cases shown in table 5.

3.2 Details of the system performance

Figure 12 shows the total heat transfer breakdown for desiccant evaporative cooling in Honolulu for the working days in a year. The building in this location needed cooling throughout the year. It can be noticed that the adsorption heating suffered little variations, and that its value is very similar to the DEC cooling one. This allowed the EC to cool the process air, see figure 3. It can also be seen that when the adsorption heat decreased, due to the lack of solar radiation, the net cooling energy also decreased. Thus, the desiccant evaporative system needed the regeneration energy over a certain value in order to work properly. In [26] it is stated that below 60 °C regeneration temperatures are considered low, although the DW studied could work with regeneration temperatures around 40 °C.

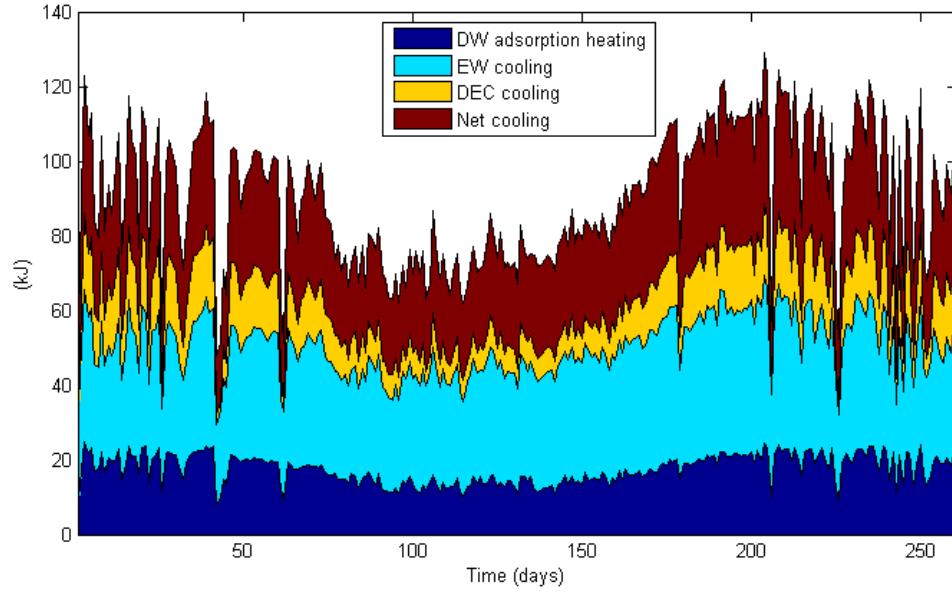


Figure 12. Energy exchange for each element in Honolulu for working days.

3.3 Annual reference heating and cooling loads

Before presenting the results of the ratio of energy demand covered using UTC's, it is convenient to examine the annual heating and cooling demand in each climate and for each building shape without using UTC-DEC system, figures 13 and 14. Vienna presented the highest heating demanding climate, whereas Honolulu did not show any heating demand at all. Athens presented a higher heating demand than Cairo. Regarding cooling demand, the greater values were found in Honolulu, Cairo and Athens, and the less demanding location was Vienna. In all climates, the compact shape showed the lowest heating and cooling energy demand, as this shape has the lowest area to volume ratio.

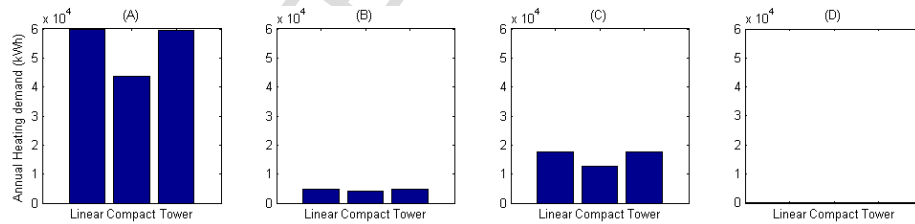


Figure 13. Heating demand without UTC façade. Climates: (A) Vienna, (B) Cairo, (C) Athens, (D) Honolulu.

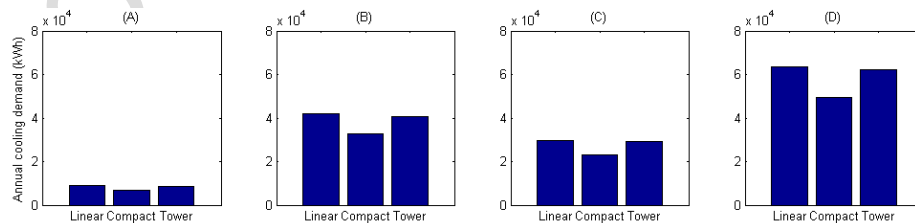


Figure 14. Cooling demand without UTC façade. Climates: (A) Vienna, (B) Cairo, (C) Athens, (D) Honolulu.

3.4 Weekly typical heating and cooling demand coverage

Figures 15 and 16 show the performance of the UTC system in the heating season for a typical winter week in the most and least heating demanding locations, Vienna and Cairo, respectively. The figures also show the incident solar radiation on the UTC façade. It can be seen that in Vienna the demand coverage during the day is lower in the morning and in the afternoon, when the sun is low in the sky and the incident angle on the south façade is small. In the case of Cairo, heating demand coverage was lower in the first hours in the morning but reach 100% at noon. However, the heating demand in Cairo was low, see figure 13, so heating demand coverage was not as critical as in Vienna. In some cases, usually first time in the morning and in the late afternoon, negative values were found, as the sun was low in the sky and its incident angle was insufficient to heat up the ventilation air. In these cases cold air was introduced into the building, thus increasing the heating demand.

Figure 16 shows that the heating demand coverage in Cairo only applies to the morning hours, since the heating demand was low in this climate, figure 13. In the afternoon, the heating demand disappears for this climate, so introducing heat air led to overheating. In the heating case, the UTC performance is like any other kind of solar collector, but it's more sensitive to wind, as convective losses to the outside depend on the wind velocity, equation 3. In order to prevent the thermal losses from increase, an adequate value of the air flow rate through the façade should be set [6].

Figures 17 and 18 show the cooling demand coverage in the most and least favourable locations for a typical summer week, Vienna and Athens. In the case of Vienna, there was a high percentage of coverage, due mainly to its low cooling demand without UTC. Athens had lower cooling demand coverage, due to its high humidity in the summer. In this case an evaporative cooling system is not as effective as in a dry climate.

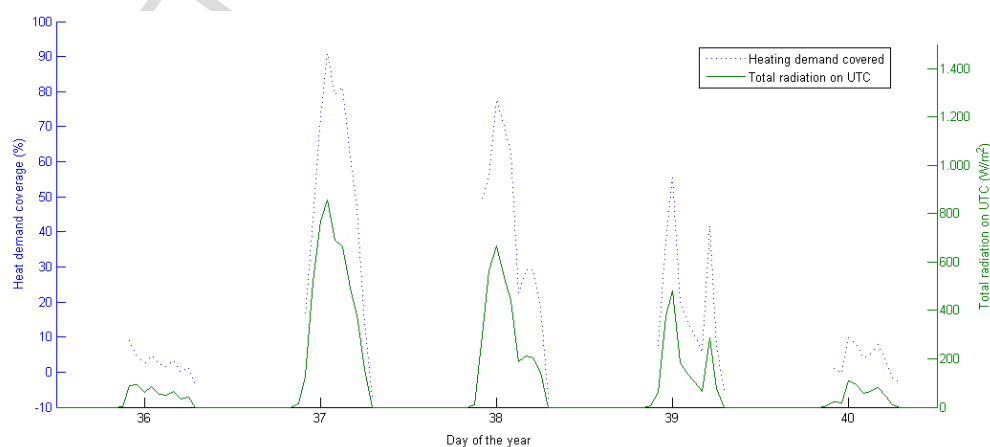


Figure 15. Heating coverage for Vienna in a typical week. South UTC facade orientation.

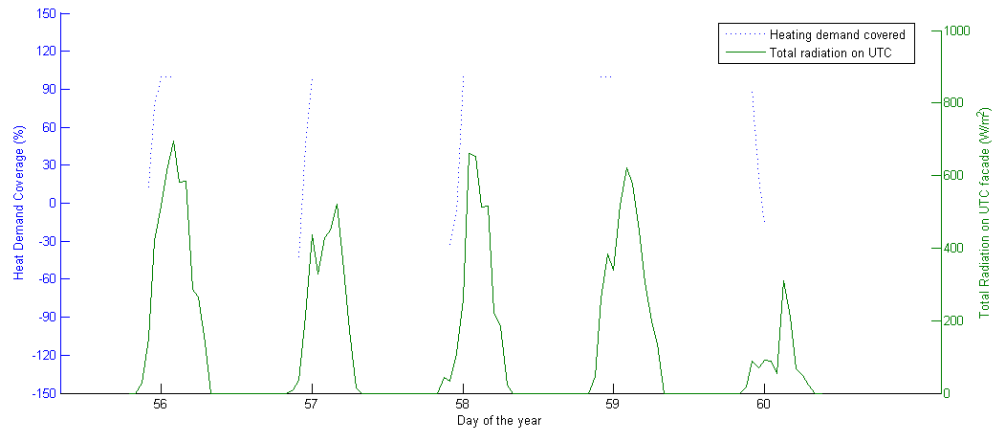


Figure 16. Heating coverage for Cairo in a typical week. South UTC orientation.

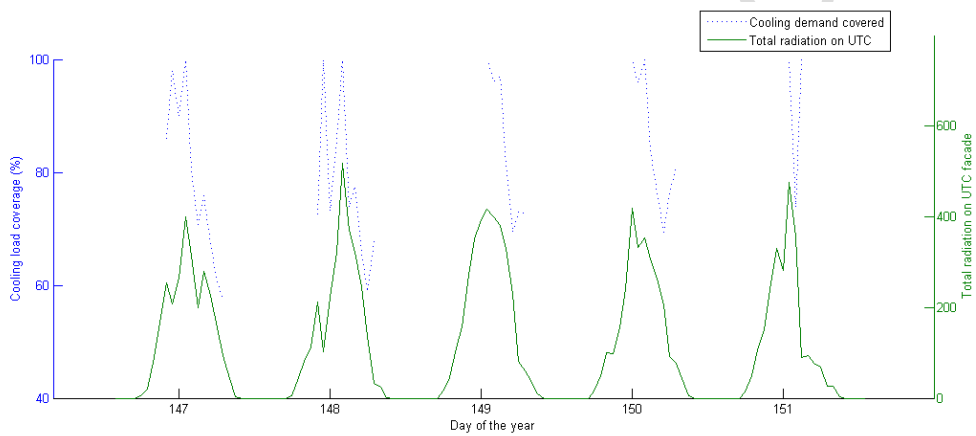


Figure 17. Cooling coverage for Vienna in a typical week. South UTC facade orientation.

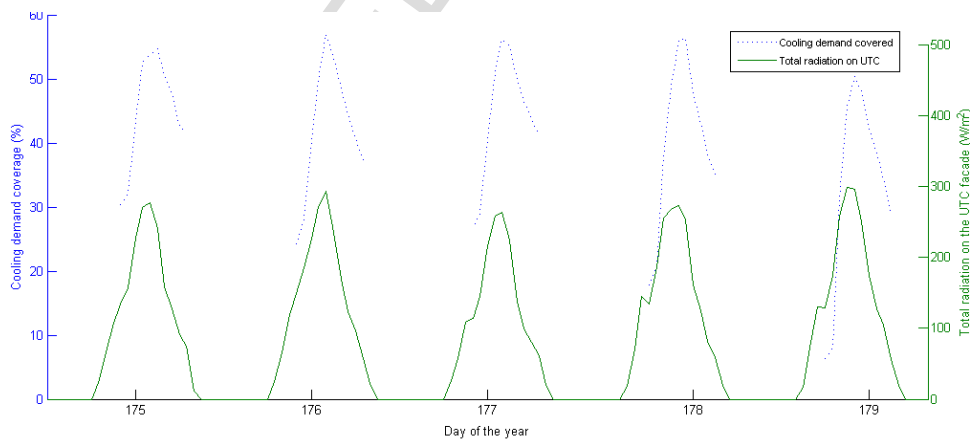


Figure 18. Cooling coverage for Athens in a typical week. South UTC orientation.

3.5 Effect of the UTC façade orientations and the building shape

The effect of UTC façade orientation on the heating and cooling demand was studied for the example of the linear building shape. The trends were found similar for the rest of shapes. Figure 19 shows the heating demand coverage and the total solar radiation in a typical winter week in Vienna. When the UTC façade was facing north the lowest heating demand coverage was

obtained, see figure 19A. The highest demand was found in the south orientation. The east and west orientation presented greater coverage during the morning and afternoon hours respectively. In all cases the heating demand coverage increased when the incident solar radiation on the façade increased, days 1 to 2, and decreased when it was decreased, days 3, 4 and 5.

Figure 20 shows the coverage of cooling demand in a typical summer week in Athens. In the north and south orientations, figure 20 A and B, an approximately 60 % of the demand was met by the DEC system at midday hours. In the east and west orientations, figure 20 C and D, the values were similar, but the peak values were displaced to the morning hours for east UTC and to the afternoon for west UTC.

These results show that the solar radiation peak values on the UTC façade and peak values of cooling demand not always coincide in time. Thus, the orientation of the façade equipped with UTC's should be carefully selected to match the energy demand. If maximum cooling energy is needed, it could be advisable to install UTC's in several orientations, achieving in this way a flatter profile. Regarding the effect of the building shape, figures 21 and 22 presents the heating demand coverage in Vienna and the cooling coverage in Athens, respectively, for the UTC south orientation.

The heating demand coverage followed the same trend as the solar radiation in all cases. The highest coverage values were found for the compact shape and the lowest values for the linear shape, see figure 21 A. In this case, a higher façade area resulted in greater heat losses, so the high surface to volume ratio shapes were penalised.

Besides, high rise buildings are more probably exposed to solar radiation than lower ones. Low rise buildings are not usually in a standalone configuration in cities, and they have more possibilities of being shaded by surrounding buildings, trees or other obstacles.

In figure 22, the case of linear shape presented a higher cooling demand coverage values than the compact and tower ones. In the compact case the reduced façade area is insufficient for activate thermally the desiccant wheel. In tower shape heating loads were higher due to larger standard facades to the east and west. Additionally, this is an example in a humid climate, so dehumidification is critical to achieve evaporative cooling. Thus, a high regeneration temperature is needed for the system to work well.

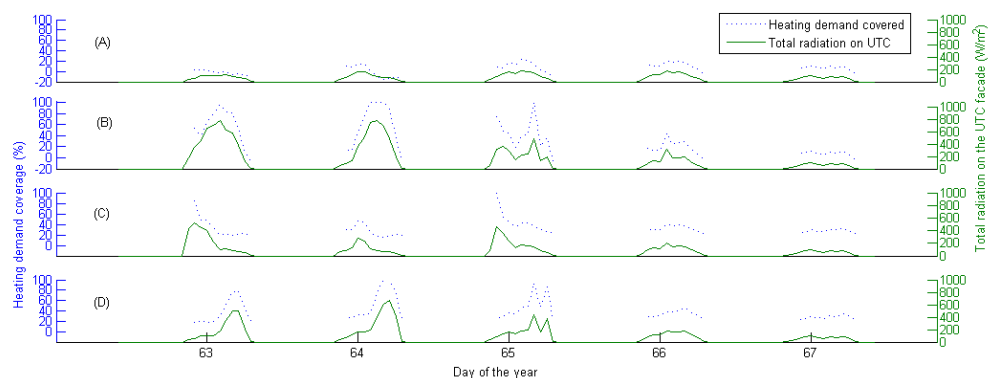


Figure 19. Heating coverage for Vienna in a typical week. Linear shape. Orientations: (A) north, (B) south, (C) east, (D) west.

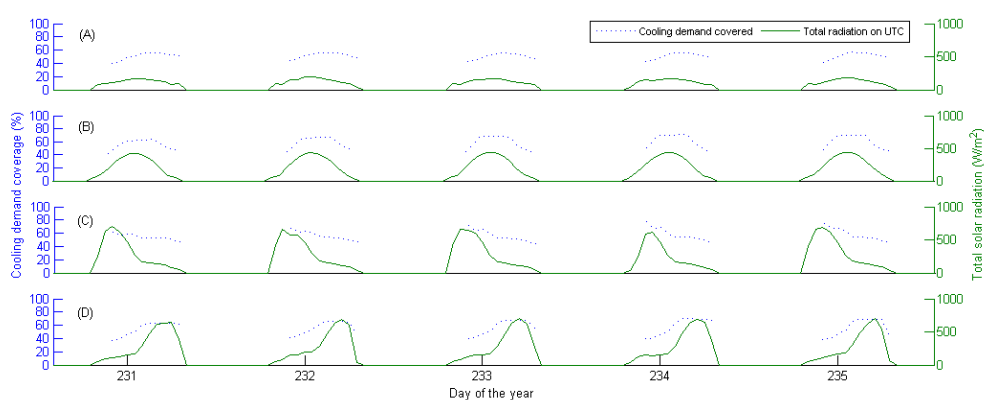


Figure 20. Cooling demand for Athens in a typical week. Linear Shape. UTC facing: (A) north, (B) south, (C) east, (D) West.

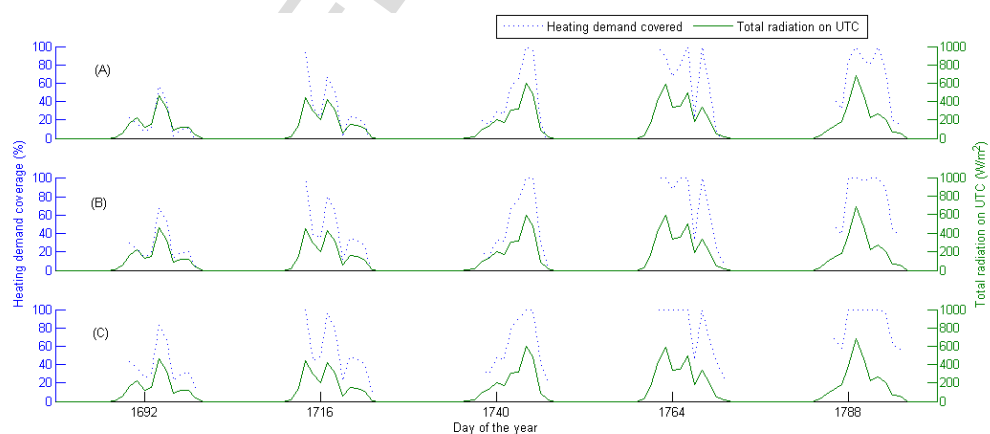


Figure 21. Heating coverage Vienna in a typical week. South UTC facade orientation. Shapes: (A) linear, (B) compact, (C) tower.

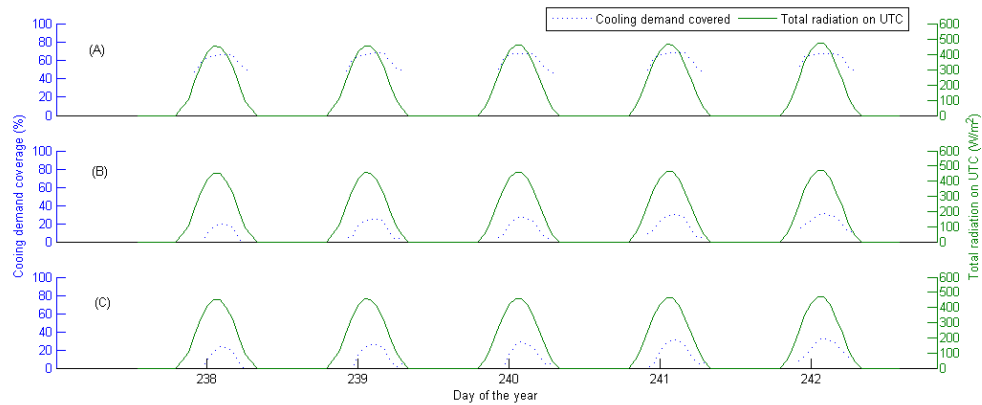


Figure 22. Cooling coverage for Athens in a typical week. South orientation. Shapes: (A) linear, (B) compact, (C) tower.

3.6 Annual heating and cooling demand coverage

3.6.1 Heating

The annual heating demand coverage values are shown in figure 23. Regarding UTC orientation, the greatest values were found for south, east and west orientation. Athens presented a maximum of 99.7 % coverage for south orientation, for compact and tower shapes. Regarding the shape, the tower cases were found to have the greater annual heating demand coverage for south orientation, whereas the linear shape presented higher values for the east and west orientations. In Cairo, positive, i.e. heating energy saving, values were found mainly for the south orientation, although the maximum value was found for west orientation, 42.0 %. The negative values, i.e. an increase in energy demand, in this case were not significant, as the heating demand for this location was very low, so any cold air introduced through the UTC caused the heating demand to increase. The highest heating coverage values were found in Athens, where, even for north orientation, covering values reached almost 100 % of the heating demand.

Figure 24 shows the SPF for the cooling season for all locations and building shapes. The highest values were found in Athens, whereas the lowest values were found in Vienna. Honolulu did not present any heating demand at all, so its SPF value is zero. Regarding the shape, the highest values corresponded to the linear building, and the best UTC orientation was found to be south, where solar radiation is higher.

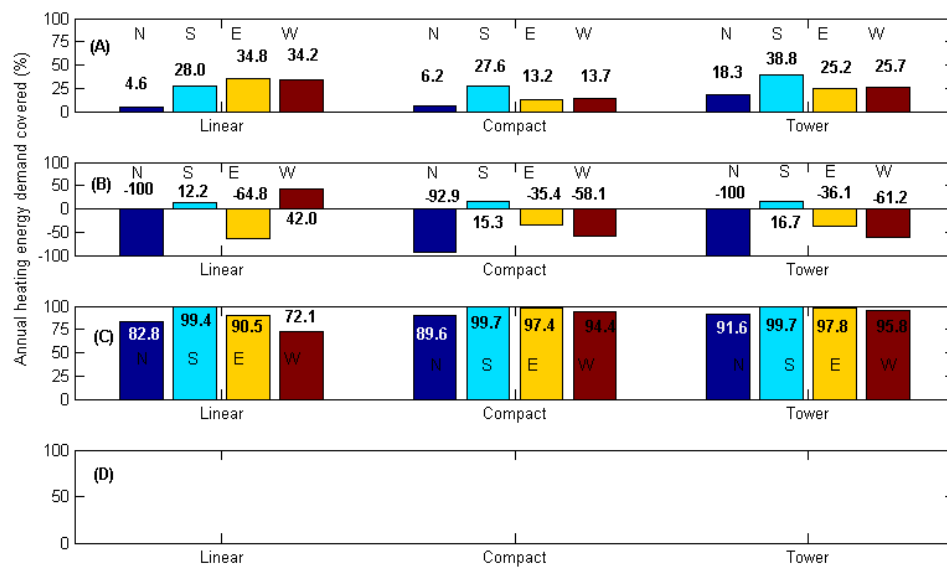


Figure 23. Annual heating demand covered by the UTC-DW-DEC system by UTC façade orientation. Locations: (A) Vienna, (B) Cairo, (C) Athens, (D) Honolulu.

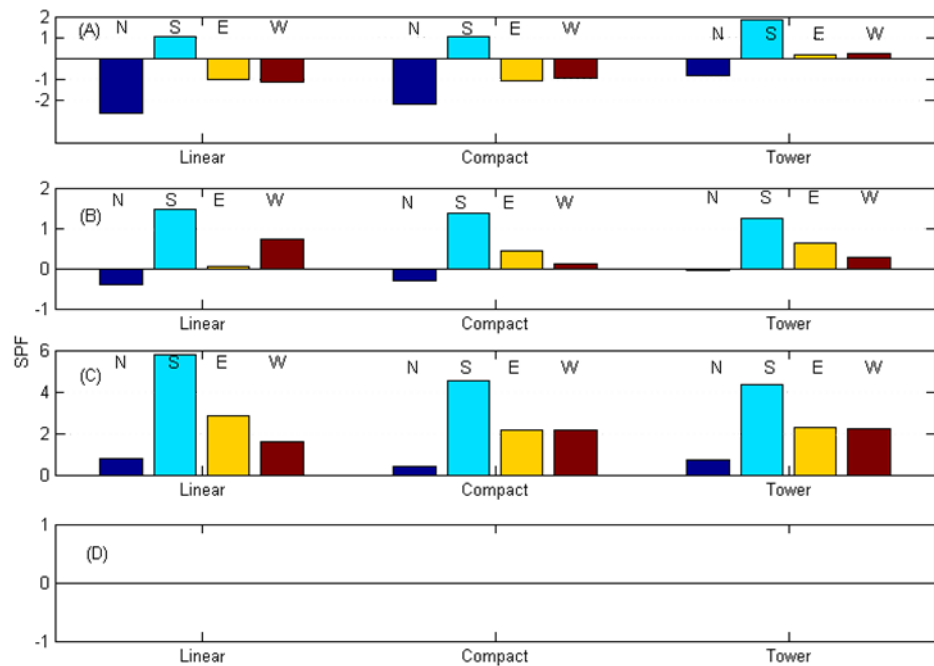


Figure 24. SPF Heating by UTC façade orientation. Locations: (A) Vienna, (B) Cairo, (C) Athens, (D) Honolulu.

3.6.2 Cooling season

Figure 25 shows that the highest annual coverage demand was found in all locations for the linear building shape. The highest value, 77.1 % was found for the linear building in Vienna. Honolulu and Athens showed similar coverage values with a maximum of 59.3 % and 50.2 % respectively. The reason is that both had very humid climate. Furthermore, Honolulu is a tropical climate and needs cooling throughout the year. Only Cairo and Honolulu had positive cooling demand coverage values for the compact and tower shapes. In the former case because of its dry climate, that is convenient for evaporative cooling, and in the latter for its milder temperatures.

All the locations presented a positive SPF value, as figure 26 shows. The lowest value was for the north orientation. The south orientation had the highest values in general, but similar values were obtained in the east and west orientations. This result showed that installing a DEC system could be an effective method for reducing cooling energy demand. Similar values were found in [35]. Higher values could have been obtained if the UTC inlet air could be connected to the outlet air stream from the RHE, but due to the structure of the UTC, it can only work with ambient air, leading to lower SPF values [6].

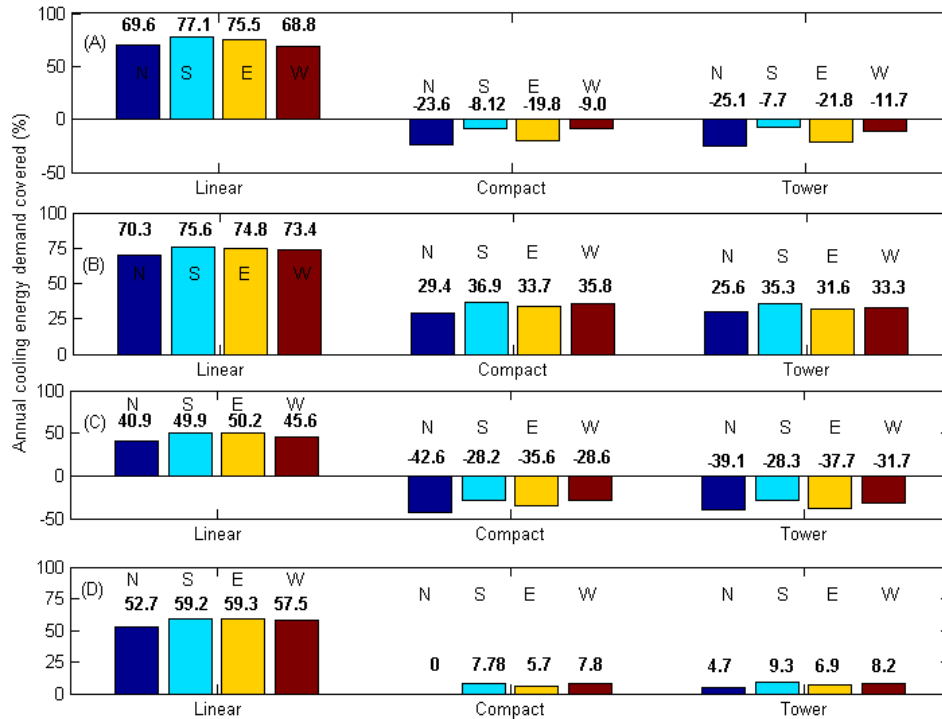


Figure 25. Annual cooling demand covered by the UTC-DW-DEC system by UTC façade orientation. Locations: (A) Vienna, (B) Cairo, (C) Athens, (D) Honolulu.

524

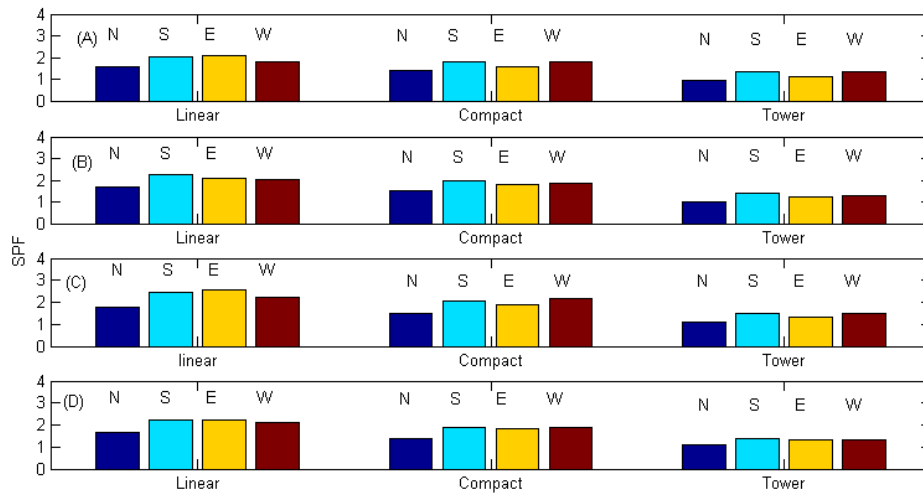


Figure 26. SPF Cooling by UTC façade orientation. Locations: (A) Vienna, (B) Cairo, (C) Athens, (D) Honolulu.

3.7 Cost analysis

Tables 6 and 7 show the simple payback period for the UTC façade in the heating and cooling system for all shapes and orientations studied. Positive values of the P_1/P_2 factor mean that the energy savings are enough to compensate for the initial investment, whereas negative values mean the expenses are greater using the UTC façade.

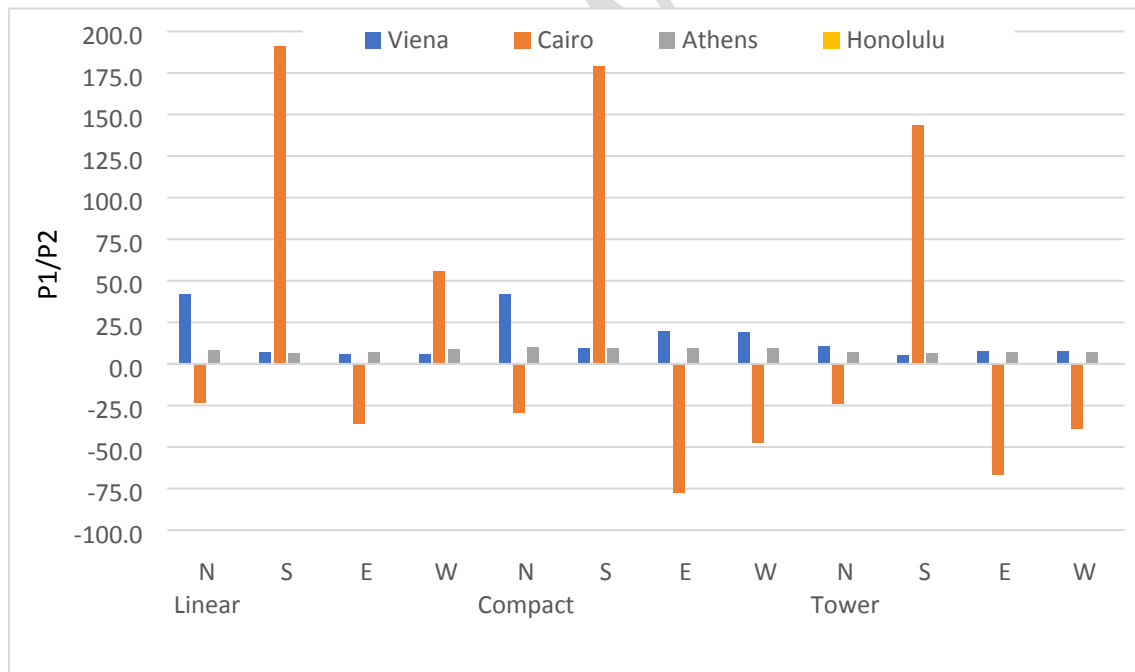


Figure 27. P_1/P_2 factor or simple payback period in years for using the UTC facade in the heating system.

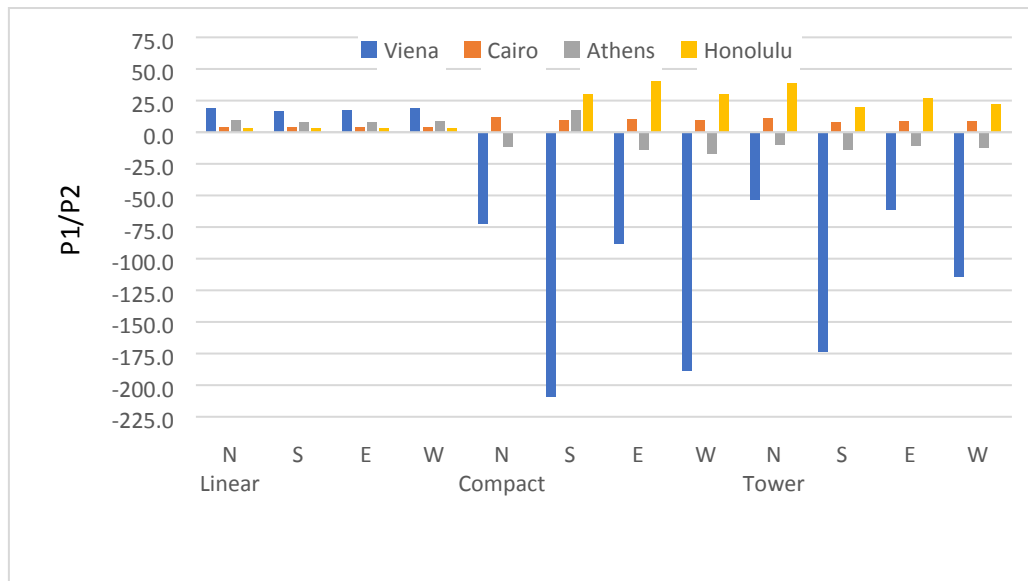


Figure 28. P_1/P_2 factor or simple payback period in years for using the UTC facade in the cooling system.

In the case of heating, Figure 27, Vienna presented the lowest payback periods for the linear shape, orientations south, east and west, and tower shape south orientation. In the case of Cairo, heating with an UTC façade is not a good investment, as their payback periods are either negative or very high. Athens can be considered a good location for installing UTC facades as the payback periods were positive in all cases with values between 6.5 and 10.1 years. In Honolulu climate there is no need for a heating system, so no payback period calculations were done.

Figure 28 shows the payback periods in the case of the cooling system. Vienna presented positive values only in the linear shape, for north, south and east orientations. In contrast, Cairo presented positive values in all cases, with payback periods around 3.5 years for the linear shape and all orientations, and relatively low values in the rest of the cases. Athens presented positive values only for the linear shape, with payback periods from 7.6 to 9.3 years. Honolulu presented positive values in all cases, except for compact shape, north orientations. However, only low values were found for the linear shape. For the rest of cases, the payback periods were higher than 19.7 years.

According to this data, Vienna and Athens climates have a high potential for energy saving using a UTC façade both with the heating and cooling system, and the linear building shape is the most adequate. On the other hand, Cairo and Honolulu's potential is only high for the cooling season, also with the linear building shape.

Summarizing, the Mediterranean climate is most appropriate to obtain heating energy savings, above 90%, using a UTC-DEC system, with compact and tower shapes having the maximum heating demand coverage values, and being south the best orientation to install the UTC façade. As for cooling, the greatest energy saving, 77.1%, was obtained in moderate climate, linear shape and south orientation, figure 25 (A).

4 Conclusions

Refurbishment of facades using unglazed solar collectors was evaluated in this paper. Heating was achieved by introducing the air directly from the UTC's modules. For cooling, a desiccant evaporative cooling system was implemented. A series of simulations were carried out under four different climate conditions, installing the UTC on the four orientations and testing it for three different building shapes.

The results showed that heating was possible in all the climates and building shapes studied, with moderate and mediterranean climates presenting a higher potential in the cost analysis. Cooling was achievable with maximum energy savings in the cases where the UTC façade was installed in the south and west orientation. The most favourable conditions were the linear building shape with the south orientation and a hot continental climate. The cost analysis results showed that installing the UTC-DEC system for cooling using the linear building shape was beneficial in all climates and orientations.

As a solution for the less favourable cases, an additional heating system could be used to supply the extra heat for the desiccant system to work properly. Using a combined UTC and DEC system reduce energy consumption both in the heating and the cooling season, but the shape of the building, the orientation of the façade refurbished, and the local climatic conditions should be carefully studied before deciding to install this system.

From the results obtained in this paper it can also be concluded that in some circumstances it could be more beneficial to install a UTC-DEC system using the maximum façade area possible regardless its orientation. An adequate control system could distribute conveniently the airstreams to obtain the maximum energy saving possible depending on the internal thermal load time distribution.

Bibliography

- [1] Directive 2012/27/EU of the European Parliament and of the Council of 25 October 2012 on energy efficiency, amending Directives 2009/125/EC and 2010/30/EU and repealing Directives 2004/8/EC and 2006/32/EC Text with EEA relevance. .
- [2] M. S. Buker and S. B. Riffat, "Building integrated solar thermal collectors - A review," *Renew. Sustain. Energy Rev.*, vol. 51, pp. 327–346, 2015.
- [3] J. Ortiz, A. Fonseca i Casas, J. Salom, N. Garrido Soriano, and P. Fonseca i Casas, "Cost-effective analysis for selecting energy efficiency measures for refurbishment of residential buildings in Catalonia," *Energy Build.*, vol. 128, no. Supplement C, pp. 442–457, 2016.
- [4] T. S. Ge, Y. J. Dai, and R. Z. Wang, "Review on solar powered rotary desiccant wheel cooling system," *Renew. Sustain. Energy Rev.*, vol. 39, pp. 476–497, 2014.
- [5] D. La, Y. Dai, H. Li, Y. Li, J. K. Kiplagat, and R. Wang, "Experimental investigation and theoretical analysis of solar heating and humidification system with desiccant rotor," *Energy Build.*, vol. 43, no. 5, pp. 1113–1122, 2011.

- [6] A. A. Pesaran and K. B. Wipke, "Use of unglazed transpired solar collectors for desiccant cooling," *Sol. Energy*, vol. 52, no. 5, pp. 419–427, 1994.
- [7] A. E. Kabeel, "Solar powered air conditioning system using rotary honeycomb desiccant wheel," *Renew. Energy*, vol. 32, no. 11, pp. 1842–1857, 2007.
- [8] M. Badami and A. Portoraro, "Performance analysis of an innovative small-scale trigeneration plant with liquid desiccant cooling system," *Energy Build.*, vol. 41, no. 11, pp. 1195–1204, 2009.
- [9] F. Chabane, N. Moummi, and S. Benramache, "Experimental study of heat transfer and thermal performance with longitudinal fins of solar air heater," *J. Adv. Res.*, vol. 5, no. 2, pp. 183–192, 2014.
- [10] E. Elgendy, A. Mostafa, and M. Fatouh, "Performance enhancement of a desiccant evaporative cooling system using direct/indirect evaporative cooler," *Int. J. Refrig.*, vol. 51, pp. 77–87, 2015.
- [11] M. Ibañez-Puy, M. Vidaurre-Arbizu, J. A. Sacristán-Fernández, and C. Martín-Gómez, "Opaque Ventilated Facades: Thermal and energy performance review," *Renew. Sustain. Energy Rev.*, vol. 79, no. Supplement C, pp. 180–191, 2017.
- [12] C. F. Kutscher, C. B. Christensen, and G. M. Barker, "Unglazed Transpired Solar Collectors: Heat Loss Theory," *J. Sol. Energy Eng.*, vol. 115, no. 3, pp. 182–188, Aug. 1993.
- [13] C. Brown, E. Perisoglou, R. Hall, and V. Stevenson, "Transpired solar collector installations in Wales and England," *Energy Procedia*, vol. 48, pp. 18–27, 2014.
- [14] R. Hall, C. Kendrick, and M. R. Lawson, "Development of a cassette-panel transpired solar collector," *ICE Energy*, vol. 167, no. EN1, pp. 32–41, 2013.
- [15] M. A. Paya-Marin, J. B. P. Lim, J. F. Chen, R. M. Lawson, and B. Sen Gupta, "Large scale test of a novel back-pass non-perforated unglazed solar air collector," *Renew. Energy*, vol. 83, pp. 871–880, 2015.
- [16] J. C. Hollick, "Unglazed solar wall air heaters," *Renew. Energy*, vol. 5, no. 1, pp. 415–421, 1994.
- [17] M. Ghadimi, H. Ghadamian, A. A. Hamidi, M. Shakouri, and S. Ghahremanian, "Numerical analysis and parametric study of the thermal behavior in multiple-skin facades," *Energy Build.*, vol. 67, no. Supplement C, pp. 44–55, 2013.
- [18] G. Quesada, D. Rousse, Y. Dutil, M. Badache, and S. Hallé, "A comprehensive review of solar facades. Opaque solar facades," *Renew. Sustain. Energy Rev.*, vol. 16, no. 5, pp. 2820–2832, 2012.
- [19] M. H. Ahmed, N. M. Kattab, and M. Fouad, "Evaluation and optimization of solar desiccant wheel performance," *Renew. Energy*, vol. 30, no. 3, pp. 305–325, 2005.
- [20] F. Comino, M. R. De Adana, and F. Peci, "First and second order simplified models for the performance evaluation of low temperature activated desiccant wheels," *Energy Build.*, vol. 116, pp. 574–582, 2016.
- [21] A. Shukla, D. N. Nkwetta, Y. J. Cho, V. Stevenson, and P. Jones, "A state of art review on the performance of transpired solar collector," *Renew. Sustain. Energy Rev.*, vol. 16, no. 6, pp. 3975–3985, 2012.

- 649 [22] N. Enteria, H. Yoshino, A. Mochida, R. Takaki, A. Satake, R. Yoshie, T. Mitamura, and S.
650 Baba, "Construction and initial operation of the combined solar thermal and electric
651 desiccant cooling system," *Sol. Energy*, vol. 83, no. 8, pp. 1300–1311, 2009.
- 652 [23] M. O'Kelly, M. E. Walter, and J. R. Rowland, "Simulated hygrothermal performance of a
653 desiccant-assisted hybrid air/water conditioning system in a mixed humid climate under
654 dynamic load," *Energy Build.*, vol. 86, pp. 45–57, 2015.
- 655 [24] G. Panaras, E. Mathioulakis, V. Belessiotis, and N. Kyriakis, "Theoretical and
656 experimental investigation of the performance of a desiccant air-conditioning system,"
657 *Renew. Energy*, vol. 35, no. 7, pp. 1368–1375, 2010.
- 658 [25] Código Técnico de la Edificación (CTE) Documento Básico de Ahorro de Energía (DB-HE)
659 2006. .
- 660 [26] F. Comino and M. Ruiz de Adana, "Experimental and numerical analysis of desiccant
661 wheels activated at low temperatures," *Energy Build.*, vol. 133, pp. 529–540, 2016.
- 662 [27] Solar Energy Laboratory UoW-M. GmbH TE, C., TESS., TRNSYS 16 Reference Manual.
663 2004. .
- 664 [28] D. La, Y. Dai, Y. Li, T. Ge, and R. Wang, "Case study and theoretical analysis of a solar
665 driven two-stage rotary desiccant cooling system assisted by vapor compression air-
666 conditioning," *Sol. Energy*, vol. 85, no. 11, pp. 2997–3009, 2011.
- 667 [29] S. Li, P. Karava, E. Savory, and W. E. Lin, "Airflow and thermal analysis of flat and
668 corrugated unglazed transpired solar collectors," *Sol. Energy*, vol. 91, pp. 297–315,
669 2013.
- 670 [30] H. Li, Y. J. Dai, Y. Li, D. La, and R. Z. Wang, "Case study of a two-stage rotary desiccant
671 cooling/heating system driven by evacuated glass tube solar air collectors," *Energy*
672 *Build.*, vol. 47, pp. 107–112, 2012.
- 673 [31] D. Q. Zeng, H. Li, Y. J. Dai, and A. X. Xie, "Numerical analysis and optimization of a solar
674 hybrid one-rotor two-stage desiccant cooling and heating system," *Appl. Therm. Eng.*,
675 vol. 73, no. 1, pp. 472–481, 2014.
- 676 [32] H. Li, Y. J. Dai, M. Köhler, and R. Z. Wang, "Simulation and parameter analysis of a two-
677 stage desiccant cooling/heating system driven by solar air collectors," *Energy Convers.*
678 *Manag.*, vol. 67, pp. 309–317, 2013.
- 679 [33] A. Preisler and M. Brychta, "High potential of full year operation with solar driven
680 desiccant evaporative cooling systems," *Energy Procedia*, vol. 30, pp. 668–675, 2012.
- 681 [34] "J. Remund, S.K., B. , METEONORM version 5.1 handbook, B. METEOTEST, Editor.
682 2004." .
- 683 [35] J. A. Duffie and W. A. Beckman, *Solar Engineering and Thermal Processes*, 3rd ed. New
684 York: John Wiley & Sons, 2006.
- 685 [36] J. M. Cejudo López, F. F. Hernández, F. D. Muñoz, and A. C. Andrés, "The optimization of
686 the operation of a solar desiccant air handling unit coupled with a radiant floor," *Energy*
687 *Build.*, vol. 62, pp. 427–435, 2013.
- 688 [37] B. W. Summers DN, Mitchell JW, Klein SA, "Thermal simulation and economic
689 assessment of unglazed transpired collector systems," *Wisconsin Energy Bureau*,
690 *University of Wisconsin, USA*. 1996.

Highlights

Using an unglazed solar collector as main source for heating and desiccant evaporative cooling system

Energy saving found in winter and summer season in all climates studied

South and west orientation are the best for installing unglazed solar collector facades

The lineal shape building is the best for a desiccant evaporative cooling system